[14]N Nuclear Quadrupole Dips in the Proton Spin-Lattice Relaxation Dispersion in the Smectic-*C* Phase of HpAB

E. Anoardo and D. J. Pusiol

Facultad de Matemática, Astronomía y Física, Universidad Nacional de Córdoba, Ciudad Universitaria, 5000 Córdoba, Argentina
(Received 19 January 1996)

Measurements of the proton spin-lattice relaxation dispersion were carefully carried out using the fast field cycling NMR technique. More than two chemically nonequivalent nitrogen nuclei were detected from the quadrupole dip spectrum. We conclude that the HpAB biaxial smectic-*C* local structure is composed of bimolecular unit cells.   [S0031-9007(96)00288-8]

Liquid crystals are compounds which exhibit simultaneously characteristics common to both isotropic liquids and solid crystals. The study of molecular orientational order and general structural properties of different mesophases is an important physical tool used for the design of technically useful materials.

The nature of local order in biaxial smectic liquid crystals has been extensively studied during the last twenty years using proton and deuteron magnetic resonances [1–9]. Nuclear quadrupole resonance (NQR) is an adequate experimental technique to study local order and molecular dynamical properties [10]. Because of the averaging of electric field gradients (EFGs), and the relative poor abundance of quadrupole nuclei in liquid crystal molecules, pure NQR spectroscopy becomes a complicated experiment. However, indirect detection of the quadrupole interaction in liquid crystals can be achieved using proton Zeeman-quadrupole cross relaxation techniques [1,11–14].

Quadrupole dips (QDs) in the proton spin-lattice relaxation dispersion $[T_1(\nu_L)]$ originate when ^{1}H additionally relaxes to the lattice through quadrupole nuclei (like ^{14}N) by level crossing [15,16]. As ^{14}N is an $I = 1$ nucleus, it presents three nuclear quadrupole levels, and the selection rules allow three transitions between these levels. For the nonzero asymmetry parameter (η) of the EFG at the quadrupole site, three QDs are expected: generally, a high frequency doublet and a low frequency singlet [10,11].

A few years ago we found QDs in the smectic phase of 4-4′-bis-heptyloxy-azoxy-benzene (HpAB: $C_{26}H_{38}N_2O_3$), as well as in several other smectic and nematic liquid crystals [11,13]. Because of both the relative low frequency of the ^{14}N QDs and the short proton spin-lattice relaxation times, it was necessary to use the fast field cycling NMR technique [17]. This experiment is similar to crossover relaxation in the laboratory frame at a fixed relaxation period [18]. We prefer to study the Larmor frequency dependence of T_1, to obtain the quadrupolar spectral density as explained in Ref. [14].

After the first works in *p*-azoxy anizole (PAA), cyanobiphenyls, and oxycyano biphenyls series [11,13], QDs found in EBBA by Dvinskikh and Molchanov [12]

had a smaller width than those mentioned above. To verify these results, new measurements were carried out in HpAB, PAA, and EBBA at Stuttgart using a new field cycling machine [19]. Results reported in that work did not agree with previous measurements. Smaller widths, shape, and different frequency dip positions are among the discrepancies.

In the present work we concentrate on high frequency dips $(\nu_L > 200 \text{ kHz})$ in the smectic-*C* (Sm-*C* of HpAB [20–22], with special care not to distort the shape and frequency of QDs. We took special care of the following: (1) *Stability and precision of the Zeeman field during the level crossing period.* Temporal variation of relaxation field B_r is expected to be observed as an extra broadening in the QD shapes. (2) *Temperature gradient along the sample.* As previously shown [13] the quadrupole coupling constant (κ) and the assymmetry parameter (η) vary substantially with temperature and, as a consequence, gradients seriously distort QDs. (3) *Purity of the sample.* Impurity molecules contribute an extra dispersion in the EFGs in the ^{14}N sites, giving an extra quadrupole resonance line broadening.

Through the $T_1(\nu_L)$ study we found the fine structure of previously unresolved QDs. The experiment is explained by the presence of three nonequivalent ^{14}N nuclei. Such NQR spectral structures are satisfactorily described by assuming that the Sm-*C* phase of HpAB is composed of bimolecular unit cells. In this Letter we report what we believe to be the first observation of this phenomenon in a liquid crystal compound.

The stability and precision of the relaxation field was tested with a second irradiation technique (Fig. 1). NMR absorption of water is detected if the relation $\gamma B_r / 2\pi = \nu_r$ is met, where ν_r is the second irradiation frequency applied during the relaxation period. Since, of course, no QD is expected for water, the quantity $2\pi \Delta\nu_r / \gamma$ extracted from the rf absorption as ν_r is conveniently scanned gives us a measure of the effective temporal distortion of B_r. This field fluctuation is about 0.2% at high frequency dip positions.

Four K-type calibrated thermocouples were located, respectively, at top and bottom, inside and outside of our

liquid crystalline sample while it was heated using air flow up to 150 °C. No gradients higher that 0.5 °C/cm were detected.

The fast field cycling NMR spectrometer is based on a specially designed air core 0.5 T low resistance electromagnet [23]. The electronics for the magnetic field switch and control were fully homemade in our laboratory [24]. The 17 MHz high field NMR transmitter receiver is a Matec model 6600. The free induction decay signal is digitized by a Biomation model 805 apparatus. The second frequency source is an Enertec Schlumberger model 4431 synthesizer pulsed by a homemade pulse programmer. The ν_r pulse is later amplified by a Marconi Instruments TF 2167 RF amplifier and a 250 W Motorola kit low frequency stage. The rf irradiation at both high and low frequencies is done on the same sample coil. A lead relay bank connects the sample coil with the respective high and low frequency resonant circuit. A personal computer controls all the main spectrometer functions: magnetic field temporal profile, pulse commands, data acquisition, data handling, sample temperature, and second frequency source. A second computer controls the security system of the spectrometer. An additional pulsed coil set is used for shimming the detection magnetic field. The Earth's magnetic field is compensated by an external dc driven Helmholtz coils pair.

T_1 was measured with an automatic acquisition of the NMR signal. Data evaluation was performed using homemade and commercial software. Commercial E. Merck (Darmstadt) HpAB was recrystalized several times from a solution with pure proanalysis ethanol, until a yellow and crystalline solid was reached. After each recrystalization step, fusion and clearing points were checked. Just before no noticeable changes on the clearing points were measured the purification process was finished.

The thermal treatment of the sample was similar to that carried out in previous experiments [11,13,19]. The sample was heated to the isotropic phase at 130 °C and maintained for about 10 min. The narrowed (liquidlike) NMR signal confirmed that the nematic-isotropic phase transition was over. Then it was cooled to the Sm-C (through nematic) phase until 82 ± 0.5 °C. The total transition process took about 45 min. Again, the proton NMR signal was used to check the respective phase transitions. The sample was left at the working temperature for about 1 h before starting $T_1(\nu_L)$ measurements. The complete thermal cycle was performed with the sample located in the probe head and the spectrometer magnetic field adjusted at 100 mT. The measurement time was about 4 days for each covered frequency interval (360–660, 750–910, 1800–4000) kHz, with the sample maintained at $T = 82$ °C. The sample purity was checked after measurements and data taken with decomposed samples were discarded. New measurements were always started with a just recrystallized HpAB sample. Experiments at several cooling times (respectively, 20, 90, and 180 min from the isotropic phase) were performed. Within experimental errors the results were found to be satisfactorily compatible.

The total Hamiltonian of the ^{14}N nuclei can be expressed by the Zeeman $\mathcal{H}_Z$ and quadrupole $\mathcal{H}_Q$ contributions [10]. In the limit of a weak Zeeman field, we had to consider the possibility that H_Z and off diagonal elements of H_Q are comparable. In this case, the high frequency resonances for $I = 1$ spin are
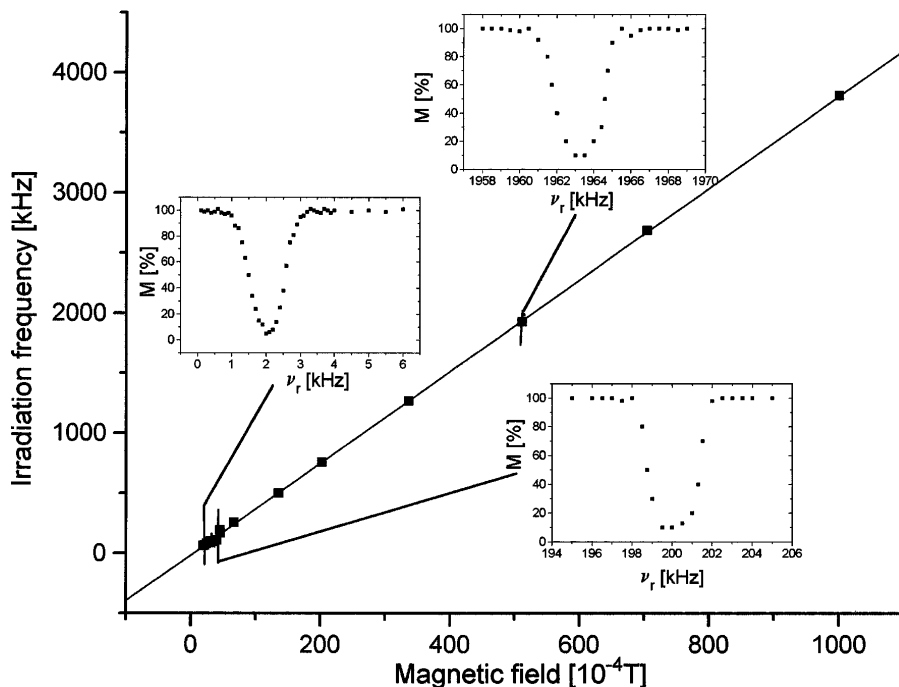

FIG. 1.   Plot of second irradiation resonance frequency vs the relaxing magnetic field for ^{1}H NMR of water. Inserts are given for three typical experiments at about $\nu_L = 2$ kHz, 200 kHz, and 2 MHz, respectively.

$$\nu_+ = \frac{1}{2\pi\hbar}\left[3A + \sqrt{(\hbar\Omega\cos\Theta)^2 + (A\eta)^2}\right],$$
$$\nu_- = \frac{1}{2\pi\hbar}\left[3A - \sqrt{(\hbar\Omega\cos\Theta)^2 + (A\eta)^2}\right], \quad (1)$$

where $A = e^2qQ/4 = \pi\hbar\kappa/2$, $\Omega = \gamma_N B_0$, and Θ is the angle between the EFG and B_0.

These expressions are valid for a monocrystalline sample. Since liquid crystal molecules are oriented with an external field due to their magnetic anisotropy [25], we consider the Sm-C mesophase surviving a thermal treatment, as described above, as a monocrystalline rather than a powder.

A rough calculation considering the extreme limit of small Θ shows that $A\eta$ and $\hbar\Omega$ are comparable. Taking into account that the occurrence of ν_+ and ν_- of each nonequivalent nitrogen is at different Zeeman external fields, we had to consider an Ω_+ and Ω_- for each line of the doublet in Eq. (2). Therefore we have

$$\nu_+ - \nu_- = \frac{1}{2\pi\hbar}$$
$$\times \left[\sqrt{(\hbar\Omega_+\cos\Theta)^2 + (A\eta)^2}\right.$$
$$\left. + \sqrt{(\hbar\Omega_-\cos\Theta)^2 + (A\eta)^2}\right] \quad (2)$$

from which we approximate

$$(\nu_+ - \nu_-)^2 \approx \frac{1}{(2\pi)^2}\left[\Delta^2\cos^2\Theta + \left(\frac{2A\eta}{\hbar}\right)^2\right], \quad (3)$$

where $\Delta^2 = \Omega_+^2 + \Omega_-^2 + 2\Omega_m^2$ with $\Omega_m = (\Omega_+ + \Omega_-)/2$. From (4) and because $A\eta = \pi\hbar\nu_0$ where ν_0 is the low frequency resonance of $I = 1$ NQR (which is not affected by the Zeeman term), we have

$$\cos\Theta = \pm\frac{2\pi}{A}\sqrt{(\nu_+ - \nu_-)^2 - \nu_0^2}. \quad (4)$$

For the present case, A can be written as

$$A = 0.206[(3/2)(\nu_+^2 + \nu_-^2) + \nu_+\nu_-]. \quad (5)$$

Finally, the values of the quadrupolar constant and the asymmetry parameter can be calculated from $\kappa = (2/3)(\nu_+ + \nu_-)$ and $\eta = 2\nu_0/\kappa$.

Table I summarizes dip frequency assignments to the three resolved nonequivalent ^{14}N and the calculated values of Θ, κ, and η for each. These results suggest that bimolecular unit cells are present in the smectic HpAB. The measured ν_0 value of nitrogen 3 was about 30 kHz [24] in near coincidence with previous data [11,13]. As can be observed in Fig. 2, the dips of 880 and 825 kHz have greater intensities than the others, suggesting that two nonresolved nitrogens could be associated to them. This result was previously found in similar liquid crystalline compounds in the solid [18]. In this reference it was clearly observed that each of the ν_0 lines of PAA and HOAB also split into three dips. Moreover, the double resonance spectra of ν_0 showed a central line with twice the intensity as the other two, corresponding to a nonresolved pair of nitrogens with the same unit cell.

The dynamical effect can also be considered. Transforming the EFG tensor from the principal system to a molecular frame with the z axis pointing along the longitudinal molecular axis, and from that frame to the laboratory, η can be expressed in terms of the Euler angles of the rotations [4]. If the molecule rotates about the longitudinal axis in a nearly unhindered fashion and fast compared with the experimental time scale, η becomes independent of the position of different nitrogens in the cell (the final expression in this limit does not depend upon the first rotation). According to this limit, η should be the same for all nitrogens of the cell. As is clear from Table I this is not the present case and it can be concluded that there exists a rotational freeze-out. This process is described in detail in Refs. [4,6,9]. Moreover, he Sm-C phase is biaxial and the free rotation of the molecule about its long axis is incompatible with the structure. As shown in Table I, the unresolved nitrogens have smaller η, and, therefore, they can be associated with the sites not bounded to the oxygen of each molecule. The other nitrogens have similar asymmetry parameters and correspond to the oxygen bonded sites.

The measured angles have reasonable values. In fact, the PAA molecule, which has the same molecular core as HpAB, has an angle of about 55° between the N═N bond and the longest molecular axis. However, the measured angle is not this one nor the tilt of the mesophase. Besides, there is no reason to suppose the N═N bond direction to be the EFG one. We expect to obtain a good approximation from quantum semiempirical molecular electrostatic maps. Results will be discussed elsewhere.

Our measurements coincide very closely (in both width and shape) with that of Zollino [19], but they did not detect the second peak in the pairs. The earliest experimental results [11,13] using an old fast field cycling spectrometer [26] show broadened QDs (about 150 kHz). Possibly, in that old spectrometer the relaxation field stabilities were not well controlled.

Discrepancies in dip frequency position are expected to depend on magnetic field homogeneity [19], thermal and magnetic field history before starting measurements, magnetic field values used in the polarization, and detection periods and purity degree of the sample. This last dis-

TABLE I. NQR parameters for HpAb in the Sm-C phase calculated from the QD analysis for three resolved nitrogens.

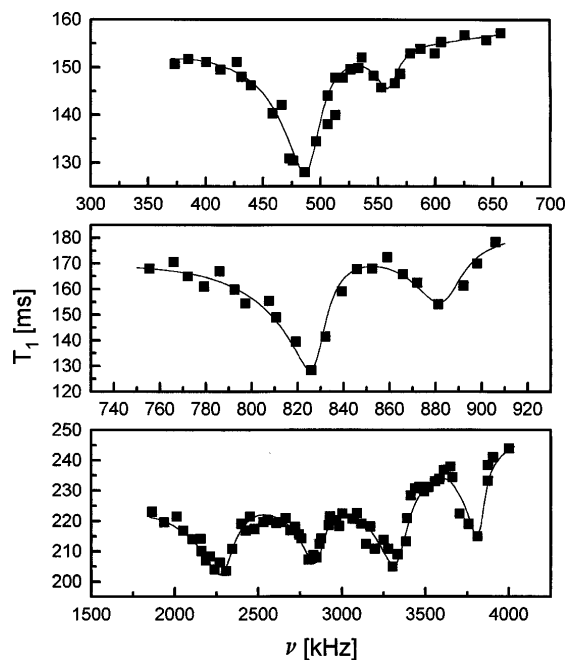|	N_1	N_2	$N_{3,4}$
ν_+ (kHz)	2840	3800	880
ν_- (kHz)	2260	3300	825
ν_0 (kHz)	560	485	30
Θ (deg)	65.9	76.3	68
κ (kHz)	3400	4733.3	1136.7
η	0.33	0.2	0.05

FIG. 2. (a) Experimental results of $T_1(\nu_L)$ in the high frequency QDs range. Eight $T_1(\nu_L)$ dips were found. The $T_1(\nu)$ dip shape is explained by the semiempirical model we described in a previous paper (solid line) [14].

crepancy remains an open issue for further research, from which new accounts of using fast field cycling NMR on liquid crystal physical properties will be reached.

Two nonequivalent molecules also can be explained by assuming an inhomogeneous sample composed of coexisting phases at the working temperature. For example, as the values of η and κ of N_1 and N_2 listed in Table I are close to the values found in solids [18], nuclei may correspond to molecules in an (monotropic) ordered smectic phase, while N_3 and N_4 have small η and κ values, typical of a rather fluid smectic-C phase. Because of (i) the above described thermal treatment of the sample (we reach the Sm-C order from the isotropic phase), (ii) the number of the detected QDs is independent of the cooling rate from the isotropic phase, (iii) the broad temperature range of the Sm-C HpAB (solid–74.5 °C–Sm-C–95.4 °C–nematic–124.2 °C–isotropic), (iv) the high purity of the sample, (v) the long time (4 days) the sample was at $T = 82$ °C during measurements, and (vi) the low temperature gradients in the sample, we believe that such possibility could be less probable.

In conclusion, if the present interpretation of bimolecular local structure of the Sm-C HpAB is realistic, and simultaneously we agree with the solid two-molecule unit cells found in similar compounds and by a similar technique [18], we could assume that the Sm-C mesophase keeps the same property from a solid, even when the Sm-C is reached from the isotropic disorder. Moreover, we conclude that the strong interaction in between the two molecules of the solid cell is not broken from the solid

to the smectic mesophases. The softening of the intercell forces is then responsible for the fluidity of the Sm-C material.

[1] J. Seliger, R. Osredkar, V. Žagar, and R. Blinc, Phys. Rev. Lett. **38**, 411 (1977).
[2] F. Volino and A. J. Dianoux, Phys. Rev. Lett. **39**, 763 (1977).
[3] J. Seliger, V. Žagar, and R. Blinc, Phys. Rev. A **17**, 1149 (1978).
[4] D. Allender and W. Doane, Phys. Rev. A **17**, 1177 (1978).
[5] R. Blinc, J. Seliger, M. Vilfan, and V. Žagar, J. Chem. Phys. **70**, 778 (1979).
[6] D. J. Photinos, P. J. Bos, and J. W. Doane, Phys. Rev. A **20**, 2203 (1979).
[7] M. Vilfan, J. Seliger, V. Žagar, and R. Blinc, Phys. Lett. **79A**, 186 (1980).
[8] N. Vaz, M. Vaz, and W. Doane, Phys. Rev. A **30**, 1008 (1984).
[9] R. Blinc, J. Dolinsek, M. Luzar, and J. Seliger, Liq. Cryst. **3**, 663 (1988).
[10] T. P. Das and E. L. Hahn, *Nuclear Quadrupole Resonance Spectroscopy* (Academic Press, New York, 1958).
[11] D. Pusiol and F. Noack, Liq. Cryst. **5**, 377 (1989).
[12] S. Dvinskikh and Y. Molchanov, Kimicheskaya Fiz. **10**, 1204 (1991).
[13] D. Pusiol, R. Humpfer, and F. Noack, Z. Naturforsch. A **47**, 1105 (1992).
[14] E. Anoardo, D. Pusiol, and C. Aguilera, Phys. Rev. B **49**, 8600 (1994).
[15] D. Woessner and H. Gutowsky, J. Chem. Phys. **29**, 804 (1958).
[16] G. Voigt and R. Kimmich, J. Magn. Reson. **24**, 149 (1976).
[17] F. Noack, Prog. Nucl. Magn. Reson. Spectrosc. **18**, 171 (1986).
[18] J. Seliger, R. Osredkar, M. Mali, and R. Blinc, J. Chem. Phys. **65**, 2887 (1976).
[19] P. Zollino, Diplomarbeit, Universität Stuttgart, 1993.
[20] D. Demus, *Flüssige Kristalle in Tabellen* (VEB Dt. Verlag der Grundstoffindustrie, Leipzig, 1976).
[21] W. Becker (Merck KGaA), Darmstadt (private comunication).
[22] H. Gruler and G. Maier, Mol. Cryst. Liq. Cryst. **23**, 261 (1973).
[23] K. H. Schweikaert, G. Osswald, and F. Noack, J. Magn. Reson. **77**, 825 (1988).
[24] E. Anoardo, E. Romero, D. Pusiol, W. Zaninetti, and C. Marqués (to be published).
[25] W. H. de Jeu and W. A. P. Claassen, J. Chem. Phys. **68**, 102 (1978).
[26] T. Mugele, V. Graf, W. Wölfel, and F. Noack, Z. Naturforsch. **35A**, 924 (1980).